

Searching for Alloy Configurations with Target Physical Properties: Impurity Design via a Genetic Algorithm Inverse Band Structure Approach

S. V. Dudiy and Alex Zunger*

National Renewable Energy Laboratory, Golden, Colorado 80401, USA

(Received 7 September 2005; published 25 July 2006)

The ability to artificially grow different configurations of semiconductor alloys—random structures, spontaneously ordered and layered superlattices—raises the issue of how different alloy configurations may lead to new and different alloy physical properties. We address this question in the context of nitrogen impurities in GaP, which form deep levels in the gap whose energy and optical absorption sensitively depend on configuration. We use the “inverse band structure” approach in which we first specify a desired target physical property (such as the deepest nitrogen level, or lowest strain configuration), and then we search, via genetic algorithm, for the alloy atomic configurations that have this property. We discover the essential structural motifs leading to such target properties. This strategy opens the way to efficient alloy design.

DOI: [10.1103/PhysRevLett.97.046401](https://doi.org/10.1103/PhysRevLett.97.046401)

PACS numbers: 71.20.Nr, 61.72.-y, 71.55.Eq, 89.75.-k

Many physical properties appear to sensitively depend on the atomic configuration. This is exemplified not only by the widely different optical and mechanical properties of the isomers of carbon (diamond vs graphite vs C_{60}), but also by markedly different properties of superlattices vs quantum wells vs random alloys of the same composition [1,2]. Indeed, with the advent of vapor-phase growth of semiconductors it is now possible to grow intentionally not only disordered alloys, but also quantum wells, superlattices with different orientations, as well as spontaneously ordered alloys, all being long-lived, device-useful (albeit thermodynamically unstable [2]) structures. The ability to position atoms at will with a STM tip [3] may ultimately lead to the creation of very general “designed structures” which are not formed by any spontaneous reaction. The sensitivity of physical properties to the particular atomic arrangement and the ability to construct atomically different structures open the question of “inverse design”, i.e., finding the atomic configuration that has a specified physical property.

An interesting case of high sensitivity of properties to configuration pertains to isolated and clustered impurities that lead to deep levels in the gap. This is exemplified by nitrogen in GaP [4–6], exhibiting states that appear as multiple sharp lines below the conduction-band minimum, as seen in absorption [4], and PL spectra [5,6]. These bound states are attributed to electron localization on single nitrogen atoms, nitrogen pairs, and higher order clusters (triplets [7], etc.). These will be referred to below as “cluster states” (CS). The high structural sensitivity of the properties of nitrogen clusters is evidenced by the results of atomistic pseudopotential calculations [7,8], which show that CS energies have a strong dependence on N atom configuration in the cluster. In particular, CS energies for nitrogen pairs can vary significantly (by up to ~ 120 meV) with a change of nitrogen-nitrogen separation within the pair, and such strong variations extend up to the

5th nearest-neighbor distance. Such calculations [7,8] also clearly indicate a nonmonotonic behavior of CS level position with pair separation. These intricate and rich behaviors result from the interference between the different conduction-band valleys (Γ , X , L) and the nitrogen impurity potential, and cannot be captured by simple models [7]. Most importantly, the variations of CS levels cannot be intuitively guessed.

Impurity atoms can be placed at will via a STM tip, as shown by Eigler *et al* [3] and by O’Brien *et al* [9]. While experimentally it is still a challenge to purposely design given impurity clusters, even a random distribution of B atoms in the $A_{1-x}B_x$ alloy manifests practically any given B_p cluster configuration with probability $\sim x^p$. Although this probability becomes smaller for higher p , it increases rapidly as we go to higher B concentrations. Predicting the properties of the many possible N_p impurity clusters in GaP is thus important for understanding $\text{GaP}_{1-x}\text{N}_p$ alloys and for impurity design in general. Furthermore, for higher order N_p clusters ($p > 2$), the dependence of their energy levels on the N-N separations results in a very large number of distinct cluster geometries. Because of large supercells required for each N cluster configuration (≥ 2000 atoms, see Ref. [7]), only a small subset of that cluster configuration space can be studied directly.

A standard approach to studying the electronic properties of alloy clusters would be to intuitively choose a small set of cluster configurations and then compute their electronic properties. This direct approach was previously used for studying N_3 triplets and N-N-N chains in Ref. [7]. Yet, such a direct approach for N_p clusters in GaP can hardly predict extremal properties (e.g., the deepest cluster level in the gap), because the special geometries can rarely be guessed intuitively, and because the physical properties critically depend on which N_p cluster configurations were examined. Indeed, it is likely that a small and arbi-

trarily chosen set of cluster configurations will miss many nontrivial cases of N clusters with interesting physical properties. In this respect, it appears desirable to pose the “inverse-design” question [10]: Instead of asking which physical properties are manifested by given atomic configurations, we can ask which configuration(s) have particularly interesting given physical properties. In particular, we ask which configurations of substitutional N_p clusters have the deepest or the shallowest impurity energy level within the GaP band gap, or the highest or lowest oscillator strength, or the highest or lowest strain energy, etc. Previously, such inverse-design propositions were posed with different degrees of implementation. For example, Werner *et al.* [11] suggested that since the probability of impact ionization in a Si-Ge alloys requires numerous stringent (momentum and energy) conservation rules, it would be desirable to search a target configuration by some (yet unspecified) form of inverse approach. But no calculation was either performed or offered. Wang *et al.* [12], have searched a small space of two compounds for the combination that provides good lattice and electronic matching, while Johannesson *et al.* [13] searched a considerable space of four-component alloys with a fixed prescribed crystal structure (fcc or bcc) for the one(s) with largest formation energies.

The early work of Franceschetti and Zunger [10] has demonstrated that for combinatorial nontrivial spaces (such as all configurations spanned by an $A_{1-x}B_x$ system with p sites) one cannot apply a direct enumeration approach, but must instead use a sampling approach that “visits” but a small fraction of the configurations, yet finds the target structure efficiently. This can be done using configurational search techniques such as simulated annealing [14] and genetic algorithm [15]. The inverse band structure (IBS) methodology of Ref. [10] involves two essential elements: the forward solver and the search algorithm, which are coupled with each other in an iterative process. The “forward solver” is a method to calculate a given physical property (e.g., band gap, strain energy, defect levels, and oscillator strength) for a given structural configuration. The “search algorithm” is a method that analyzes the information generated by the forward solver and tells the forward solver which structures should be calculated next in a search for the structure possessing the target property.

We illustrate here impurity design by considering the following basic physical properties: (a) the impurity-induced strain energy (which determines their solubility), (b) the lowest energy valence-to-impurity optical transition, and (c) the oscillator strength of the above noted transition. The last two properties decide the optical properties of the impurity states. To model N_p clusters we take a large, (1728 atom) cubic supercell of GaP, and within this supercell we consider a cubic 126-atom subcell in which we place p nitrogen atoms ($p = 2-5$) substitutionally on the anion sublattice. The rest of the GaP supercell shelters

the N_p cluster from interactions with its periodic images. We then apply the valence force field method (VFF) [16] to relax the atomic positions and thus calculate the strain energy for a given N_p cluster configuration. We use the empirical pseudopotential method [7,8] and we efficiently solve [17] the single-particle atomistic Schrödinger equation to obtain the CS energies and atomistic wave functions, which are then used to calculate the dipole matrix elements (oscillator strength).

To illustrate the complexity of the relationship between the physical properties and the atomic configuration in the challenging Ga(P,N) system we selected, we show in Fig. 1 an overall map of the transition energies and the dipole transition matrix elements squared for excitations from the valence band maximum (VBM) to the lowest CS state of the various possible configurations of the N_2 , N_3 , N_4 , and N_5 clusters realizable in the above described 1728 atom GaP supercell. We see that the multitude of possible optical transitions span a wide range of energies and transition amplitudes, and increases considerably as we move from nitrogen pairs [Fig. 1(a)] to triplets [Fig. 1(b)], and especially to higher order N_p clusters with $p = 4$ [Fig. 1(c)] and $p = 5$ [Fig. 1(d)]. This demonstrates the need for a powerful search algorithm that would be able to efficiently navigate in such a complex space of properties.

In this work we use, as a search algorithm, the genetic algorithm [15,18] (GA). We represent atomic structures (“genomes” or “individuals”) as strings of integer numbers (“genes”), which list the atomic numbers of species (N or P) occupying the 63 (enumerated) anion sites in the above described subcell. We define “fitness” of an individual as a difference between the calculated value of a given physical property for that individual and the desired

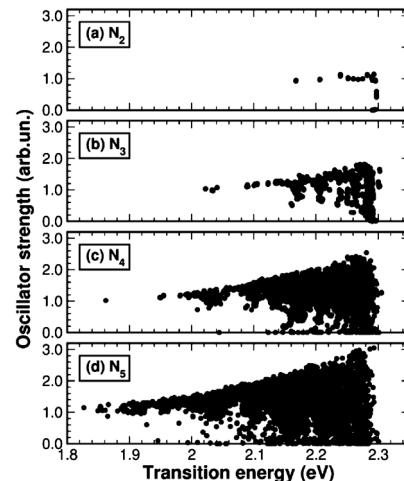


FIG. 1. The absorption strength (oscillator strength) for transitions from the GaP valence band maximum (the zero of energy) to the deepest nitrogen cluster levels produced by various configurations (dots) of clusters N_p containing p nitrogen atoms, with $p = 2-5$ [(a)–(d)]. The conduction-band minimum is at 2.355 eV. Note the wide spread in transition energies and intensities created by various configurations.

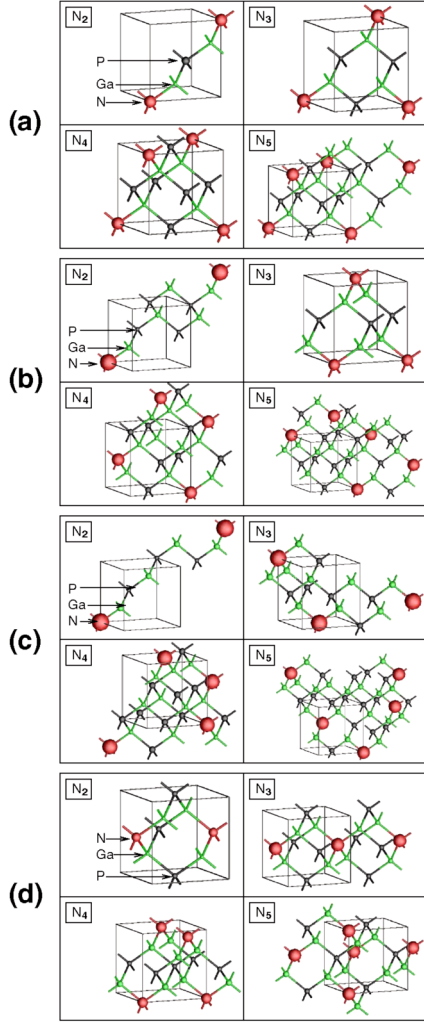


FIG. 2 (color online). Configuration of N_p clusters ($p = 2-5$) in GaP that are found to have (a) the deepest defect level in the gap, (b) the shallowest level in the gap, (c) the highest oscillator strength, and (d) lowest strain energy.

target value. We execute the GA search via the IAGA code [19], which utilizes the PGAPack library [20]. Further implementation details can be found in Ref. [21]. In all our calculations, we start with an initial population of $N_{\text{pop}} = 150$ randomly generated structures (genomes),

and then replace $N_{\text{rep}} = 31$ least fit genomes at each generation, using uniform crossover rate and mutation probability [18,21] of 0.25 and 0.03, respectively. We allow each GA run to continue for 40 generation (1360 property evaluations in total). At so many generations our population typically finishes its most explorative phase and does some refining of the fittest structures [22]. With the chosen GA settings, in a search for minimum VFF strain energy of a N_4 cluster, 7 out of 15 independent test runs find the configuration with the absolute minimum of the strain energy. Note that if instead of a GA run we would take a set of 1360 configuration chosen at random we would have only ~ 0.06 probability to capture that absolute minimum strain energy configuration. We used those GA settings to search for maximum and minimum value for each of the three properties we study, and for each N_p cluster order $p = 2-5$, performing one GA run for each of those 24 cases.

The final configurations exhibiting our target properties for most of the considered target cases are depicted in Fig. 2. While this figure conveys the full configurational elements (pairs, many-body motifs) of each structure, it is interesting to observe what type of nitrogen-nitrogen pairs lead to a given target property. This is summarized in Table I. We number there only the anion fcc sublattice and denote by nn1, nn2, ..., nn13 the first, second, and 13th nearest-neighbor (nn) nitrogen pairs occurring within clusters N_p of p nitrogen atoms. We see, for example, that if we have only two nitrogen atoms (N_2) then the minimum strain is achieved by a second nearest-neighbor (nn2) arrangement, whereas the maximum oscillator strength is achieved when the two nitrogens are 13th nearest neighbor (nn13) to each other.

Figure 2 and Table I reveal the main pair motifs responsible for given target properties. We see that: (i) Minimum strain requires the nn2 motif, but maximum strain requires the nn1 motif. (ii) Minimum VBM-to-CS transition energy (E_g) requires the nn4 motif, whereas maximum transition energy requires the nn3 one (except for the N_2 case). (iii) Maximal transition strength requires the nn3 and nn7 motifs (with a notable exception of the N_2 case with just nn13). While future detailed investigation of the mechanisms leading to these surprising motifs may reveal inter-

TABLE I. The pair motifs nnq that characterize given target property for clusters N_p of p nitrogen atoms in GaP. The properties include minimum (Min) or maximum (Max) of strain energy, E_{vff} , optical transition energy from the valence band maximum to the lowest energy cluster state, E_g , and the oscillator strength, f , of such transition. Here nnq is the q th nearest-neighbor nitrogen-nitrogen separation (in the anion fcc sublattice), and $m \times nnq$ denote m such separations.

Target	N_2	N_3	N_4	N_5
Min E_{vff}	nn2	$2 \times \text{nn2}$; nn8	$2 \times \text{nn2}$; $4 \times \text{nn3}$	$3 \times \text{nn2}$; $4 \times \text{nn3}$; $2 \times \text{nn7}$; nn8
Max E_{vff}	nn1	$2 \times \text{nn1}$; nn4	$6 \times \text{nn1}$	$5 \times \text{nn1}$; nn3; $2 \times \text{nn4}$; nn7; nn9
Min E_g	nn4	$3 \times \text{nn4}$	$6 \times \text{nn4}$	$8 \times \text{nn4}$; nn8; nn12
Max E_g	nn11	nn2; $2 \times \text{nn3}$	$4 \times \text{nn3}$; $2 \times \text{nn5}$	$5 \times \text{nn3}$; $2 \times \text{nn5}$; nn6; nn7; nn13
Min f	nn5	nn2; $2 \times \text{nn9}$	$2 \times \text{nn1}$; nn2; $2 \times \text{nn5}$; nn10	$2 \times \text{nn2}$; $2 \times \text{nn8}$ $2 \times \text{nn9}$; $2 \times \text{nn10}$; $2 \times \text{nn13}$
Max f	nn13	nn3; nn7; nn13	$3 \times \text{nn3}$; $3 \times \text{nn7}$	$4 \times \text{nn3}$; $3 \times \text{nn7}$; nn10; nn11; nn13

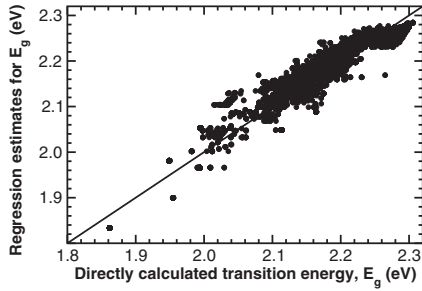


FIG. 3. Estimates from Eq. (1) versus the corresponding directly calculated values of valence-to-defect optical transition energies for all N_4 cluster geometries encountered in the present work [Fig. 1(c)].

esting physics or chemistry, the sheer identification of these and other recurring motifs (inspect Fig. 2 and Table I) out of an astronomic number of possibilities may provide in the future the necessary physical intuition needed for establishing “design” rules of materials with such target properties.

Having identified the critical areas of configuration space where our system properties are extremal, we are now in a position to learn about the overall structure-property relationship in our systems. In particular, we can take all the structure-property information we have accumulated near various extremal physical properties and “interpolate” such information to the rest of the configuration space, between those extremes, using a data mining approach. Let us take, as an example, the optical transition energy E_g for N_p clusters. As discussed above (viz. Table I), the configurations with extremal transition energy (Fig. 2) suggest possible correlation between the optical gap and the number of various nearest-neighbor pairs occurring within an N_p cluster. To investigate such correlations we apply multiple linear regression technique [23], using as predictor variables the numbers of occurrences m_q of various q th nearest-neighbor pairs (nnq motifs) within a given N_p cluster. In particular, we model E_g as a linear function of structural parameters m_q of the cluster, as $E_g \approx \sum_q a_q m_q$. We obtain the regression coefficients a_q using the method of least squares to minimize the error between the regression estimates and the actual data. For example, for $p = 4$ and $q = 1, 2, 3, 4$, we get the following expression for the optical gap (in units of meV) as a function of the N_4 cluster configuration:

$$E_g \approx 223 - 30m_1 + 7m_2 + 10m_3 - 66m_4 + 5m_5 + 0.3m_6. \quad (1)$$

The overall accuracy of this expression is described by Fig. 3. Equation (1) is seen to capture the overall trends in the property-structure relationship in this case. Moreover, from the coefficients of that equation we can gauge the relative contribution of different N-N separations within the cluster.

In conclusion, we have shown how the IBS approach [10] can be applied to efficiently explore the structure-energy relationships in a complex system, taking as an example the nontrivial case of N_p impurity clusters in GaP. The present strategy can be used to efficiently investigate such relationships in other complex systems, such as those encountered in alloy design.

This work is supported by the U.S. Department of Energy, SC-BES-DMS Contract No. DEAC36-98-GO10337.

*Electronic address: alex_zunger@nrel.gov

- [1] Landolt-Börnstein, Group III Condensed Matter, Vol. 34 (Springer-Verlag, Berlin, 2001).
- [2] A. Zunger and S. Mahajan, in *Handbook on Semiconductors*, edited by S. Mahajan (Elsevier Science, Amsterdam, 1994), Vol. 3, p. 1399.
- [3] D.M. Eigler and E.K. Schweizer, *Nature (London)* **344**, 524 (1990).
- [4] D.G. Thomas, J.J. Hopfield, and C.J. Frosch, *Phys. Rev. Lett.* **15**, 857 (1965).
- [5] J.N. Baillargeon *et al.*, *Appl. Phys. Lett.* **60**, 2540 (1992); S. Miyoshi *et al.*, *Appl. Phys. Lett.* **63**, 3506 (1993).
- [6] Y. Zhang *et al.*, *Phys. Rev. B* **62**, 4493 (2000); I.A. Buyanova *et al.*, *Appl. Phys. Lett.* **80**, 1740 (2002).
- [7] P.R.C. Kent and A. Zunger, *Appl. Phys. Lett.* **79**, 2339 (2001); *Phys. Rev. B* **64**, 115208 (2001).
- [8] L. Bellaiche, S.-H. Wei, and A. Zunger, *Phys. Rev. B* **54**, 17568 (1996); **56**, 10233 (1997); T. Mattila, L.-W. Wang, and A. Zunger, *Phys. Rev. B* **59**, 15270 (1999).
- [9] J.L. O’Brien *et al.*, *Phys. Rev. B* **64**, 161401 (2001).
- [10] A. Franceschetti and A. Zunger, *Nature (London)* **402**, 60 (1999).
- [11] J.H. Werner, S. Kolodinski, and H.J. Queisser, *Phys. Rev. Lett.* **72**, 3851 (1994).
- [12] T. Wang *et al.*, *Phys. Rev. Lett.* **82**, 3304 (1999).
- [13] G.H. Johansson *et al.*, *Phys. Rev. Lett.* **88**, 255506 (2002).
- [14] S. Kirkpatrick *et al.*, *Science* **220**, 671 (1983).
- [15] D.E. Goldberg, *Genetic Algorithms in Search, Optimization, and Machine Learning* (Addison-Wesley, Reading, MA, 1989).
- [16] P. Keating, *Phys. Rev.* **145**, 637 (1966).
- [17] L.-W. Wang and A. Zunger, *J. Chem. Phys.* **100**, 2394 (1994).
- [18] D. Levine, *User’s Guide to the PGAPack Parallel Genetic Algorithm Library*, Argonne National Laboratory, Argonne, Illinois Tech Report No. ANL-95/18, 1996.
- [19] K. Kim and W.B. Jones, computer code IAGA, 2003.
- [20] D. Levine, *Parallel Genetic Algorithm Library* (1998).
- [21] K. Kim, P. Graf, and W.B. Jones, *J. Comput. Phys.* **208**, 735 (2005).
- [22] See EPAPS Document No. E-PRLTAO-97-004630 for GA run example. For more information on EPAPS, see <http://www.aip.org/pubservs/epaps.html>.
- [23] J. Han and M. Kamber, *Data Mining: Concepts and Techniques* (Morgan Kaufmann, San Francisco, 2000).